〈Original article〉

Properties of *Geobacillus stearothermophilus* malate dehydrogenase used as a diagnostic reagent and its characterization by molecular modeling

Yoshiaki Nishiya and Yuya Shimozawa

Summary Malate dehydrogenase (Mdh) is used in assays of glutamate oxaloacetate transaminase (aspartate aminotransferase) activity and determination of bicarbonate in serum and L-malate in foods. We previously reported the development and structural analysis of a thermostable Mdh from *Geobacillus stearothermophilus* (formerly *Bacillus stearothermophilus*). The enzyme, designated gs-Mdh, is now in commercial use. Here, we conducted a detailed comparison of the enzymatic properties of gs-Mdh and other commercially available Mdhs. gs-Mdh exhibited the highest substrate affinity and thermal stability, properties desirable in a diagnostic reagent. The excellent suitability of gs-Mdh for use in transaminase assays was demonstrated by simple simulations of sequential enzyme reactions. To further characterize the properties of gs-Mdh, three-dimensional molecular models were constructed by homology modeling using the amino acid sequence revised in this study. Open- and closed-type models using base structures from *B. anthracis* and *Chloroflexus aurantiacus* were compared with other Mdh models. The outstanding structural properties of gs-Mdh in stability and activity are also discussed.

Key words: malate dehydrogenase, substrate affinity, rate assay simulation, thermal stability, three-dimensional structure

1. Introduction

Malate dehydrogenase (EC 1.1.1.37; L-malate: NAD^+ oxidoreductase, abbreviated Mdh) catalyzes the reversible reduction of oxaloacetate, using reduced β-nicotinamide adenine dinucleotide (NADH) as a coenzyme. Mdh is a key enzyme in the TCA cycle and plays important metabolic roles in aerobic energy-production pathways. The structure-function relationship of this enzyme has been studied by X-ray crystallographic analyses and protein engineering[1-6]. The three-dimensional structure and catalytic mechanism of Mdh are highly similar to lactate dehydrogenase (EC 1.1.1.27; L-lactate: NAD^+ oxidoreductase, abbreviated Ldh), which catalyzes the reversible reduction of pyruvate, using NADH as a coenzyme. Evolutionary analyses of Mdh and Ldh demonstrated that the enzymes are closely related[1,2]. Site-directed mutagenesis studies showed that enzymes exhibiting Ldh specificity can be easily converted to Mdhs by substituting only one

Department of Life Science, Setsunan University, 17-8 Ikeda-Nakamachi, Neyagawa, Osaka 572-8508, Japan.

Received for publication February 2, 2016
Accepted for publication March 28, 2016

amino acid in the substrate-binding site (glutamine to arginine)[7-11].

Mdh is useful for the clinical determination of glutamate oxaloacetate transaminase [GOT, also known as aspartate aminotransferase (AST)] and bicarbonate in serum by coupling with related reagents. Mdh is also utilized in the determination of L-malate in various foods. The Mdhs from *Sus scrofa* (pig) mitochondria, *Thermus flavus* (extremely thermophilic bacterium), and the moderately thermophilic bacterium *Geobacillus stearothermophilus* (formerly *Bacillus stearothermophilus*) (pm-Mdh, tf-Mdh, and gs-Mdh, respectively) are commercially produced and utilized as diagnostic reagents. The high substrate affinity of gs-Mdh and its stability in the diagnostic reagent for glutamate oxaloacetate transaminase make this enzyme ideal for clinical applications[12]. However, to date, no reports describing detailed analyses of the enzymatic properties of commercially available Mdhs or comparisons of their activities have been published.

We previously reported the results of structural studies of substrate-bound gs-Mdh[13], based on the deduced amino acid sequence determined from the DNA sequence of the cloned gene (DDBJ accession number: E10715). However, the three-dimensional structural model of gs-Mdh constructed by homology modeling was of poor quality by current standards because of an extremely low sequence identity (approximately 30%) with the base pm-Mdh[13]. The sequence of the C-terminal region of gs-Mdh was, moreover, revised in this study (DDBJ accession number: LC100138), because sequence errors were found. In contrast to gs-Mdh, thorough X-ray crystallographic studies of both pm-Mdh and tf-Mdh have provided complete structural descriptions of these enzymes[14,15].

In this study, we compared the enzymatic properties of pm-Mdh, tf-Mdh, and gs-Mdh in detail. Based on their kinetic parameters, the suitability of each enzyme for use in the transaminase assay was assessed based on sequential enzyme reactions. To enhance understanding of the properties of gs-Mdh, open (apo) and closed (substrate-bound) molecular models were constructed by homology modeling using base structures with higher sequence identities. The unique enzymatic properties of the enzyme were clearly elucidated based on these structural comparisons. The gs-Mdh structures described here provide a reasonable starting point for analysis of the enzyme's structure-function relationship.

2. Materials and methods

Materials

Compounds and reagents were purchased from Nacalai Tesque (Kyoto, Japan) or Wako Pure Chemical Industries (Osaka, Japan).

Enzyme preparation

Commercial enzymes were obtained from Toyobo (Osaka, Japan) and Amano Enzyme (Nagoya, Japan).

Enzyme assay

Mdh activity was assayed spectrophotometrically. One unit was defined as the amount of enzyme necessary to oxidize 1 μmole of NADH per minute under the conditions described below. The final reaction mixture contained 100 mmol/L potassium phosphate (pH 7.5), 0.5 mmol/L oxaloacetate, and 0.2 mmol/L NADH. Disappearance of NADH was measured at 340 nm and 30°C for 3 to 4 min.

Rate assay simulation

Rate assays of GOT with pm-Mdh, tf-Mdh, and gs-Mdh were simulated using Microsoft Excel. Increases in the amount of oxaloacetate and decreases in the amount of NADH were characterized based on Michaelis-Menten kinetics. Both amounts and concentrations were calculated every 0.1 sec.

Sequencing

Plasmid DNA encoding the gs-Mdh gene was purified from a culture of recombinant *Escherichia coli* JM109 grown to stationary phase in LB broth at 30°C with agitation at 180 rpm, and the gene was directly sequenced. The gene and flanking region

sequences were analyzed using GENETYX software (Software Development Co., Ltd., Tokyo, Japan).

Homology searching

Homology searching and multiple alignment of Mdh amino acid sequences were performed using MOE (Chemical Computing Group Inc., Montreal, Canada) and GENETYX software, respectively.

Molecular modeling

Models of gs-Mdh were constructed by homology modeling. Open- and closed-type three-dimensional protein models were generated using MOE software, based on structures of Mdhs from *B. anthracis* and *Chloroflexus aurantiacus* (PDB ID: 3tl2a and 1uxia), respectively. MOE and Pymol software were used for molecular visualization.

3. Results

Comparison of enzymatic properties

The detailed enzymatic properties of gs-Mdh, including the K_m value for oxaloacetate and temperature and pH profiles, were investigated and compared with those of pm-Mdh and tf-Mdh (Table 1). The K_m of gs-Mdh was much lower than that of the other enzymes, and the temperature stability of gs-Mdh was the same as that of tf-Mdh but much greater than that of pm-Mdh. Accordingly, gs-Mdh exhibited the highest substrate affinity and thermal stability among commercially available Mdhs and exhibited the highest stability in the diagnostic reagent used for GOT (e.g., the gs-Mdh, tf-Mdh, and pm-Mdh activity remaining after storage at 40°C for

Table 1 Comparison of commercially available malate dehydrogenases

Origin	K_m for Oxaloacetate (μmol/L)	Optimal Temperature (°C)	Optimal pH	Thermal Stability (°C)	pH Stability
Geobacillus stearothermophilus	5.0	70	8.0	≦70	3-9
Sus scrofa (pig) Mitochondria	33	50	8.0	≦30	7-9
Thermus flavus	68	90	8.0	≦70	3-11

Temperature activity, in 0.1 mol/L potassium phosphate buffer (pH 7.5); pH activity, in 0.1 mol/L buffer solution (pH 5-8, phosphate; pH 8-9, borate) at 25°C; thermal stability, 15 min-treatment with 0.1 mol/L potassium phosphate buffer (pH 7.5); pH stability, 20 hr-treatment with Britton-Robinson buffer at 25°C.

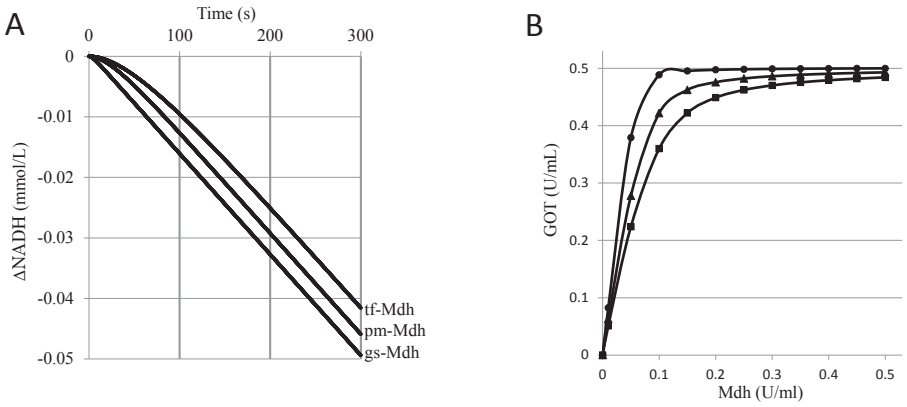

Fig.1 Simulation of rate assays of GOT with gs-, pm-, and tf-Mdh. It was assumed that the assay reagents contained various concentrations of enzyme (270 μL) and the GOT samples (30 μL) were mixtured and incubated at 30°C and pH 7.5 for 5 minutes. (A) Comparison of time courses of rate assays. Both of the assumed Mdh and GOT activities are 100 mU/mL. (B) Dose-response curves of Mdhs (gs-Mdh, circle; pm-Mdh, triangle; tf-Mdh, square) in the assay reagents. The assumed GOT activity in the sample is 500 mU/mL.

1 week was estimated as 94, 85, and 0%, respectively [data not shown]). These properties of gs-Mdh make it ideally suited for clinical applications.

Simulation of GOT assays

To examine the influence of substrate affinity on the enzymatic assays, we simulated the rate of GOT assays using gs-Mdh, tf-Mdh, and pm-Mdh (Fig. 1A). The kinetic parameters of each enzyme with respect to oxaloacetate were used in the simulations. Simple calculations of the sequential enzyme reactions demonstrated the excellent suitability of gs-Mdh for the GOT assay. The estimated minimum amount of gs-Mdh required was markedly lower than that of the other enzymes. To obtain the same results, approximately one-fifth or less of gs-Mdh would be required compared with pm-Mdh or tf-Mdh, in agreement with the K_m values of enzymes (Fig. 1B).

Amino acid sequence comparison

Structural analyses are necessary to fully understand the enzymatic properties of gs-Mdh. However, the closed form of the tertiary structure model of gs-Mdh previously constructed by homology modeling[13] was not very reliable because of the low (only 30%) sequence identity with the base pm-Mdh structure. tf-Mdh could not be used as a base structure because of extremely low sequence homology with gs-Mdh (approximately 20% identity). In addition, the C-terminal region of the gs-Mdh sequence was revised in this study because errors were found when it was re-sequenced. Construction of three-dimensional molecular models by homology modeling using the revised amino acid sequence (correct C-terminal sequence: KAALAKSVESVKNVMRMLE, former C-terminal sequence:KARSPNPSNPLKMSCACWNSGEAKIP ALPGFLSHSQ) was attempted again. As the first step in the model-building process, we re-investigated the degree of amino acid sequence homology between gs-Mdh and Mdh/Ldh family enzymes, the structures of which have been well-characterized by X-ray crystallography. As shown in Figure 2, the sequence of gs-Mdh exhibited an extremely high

```
ba-MDH   1:SNAMTIKRKKVSVIGAGFTGATTAFLLAQKELADVVLVDIPQLENPTKGKALDMLEASPV 60
gs-MDH   1:    AMKRKKISVIGAGFTGATTAFLLAQKELGDVVLVDIPQLENPTKGKALDMLEASPV 56
ca-MDH   1:      MRKKISIIGAGFVGSTTAHWLAAKELGDIVLLDI—VEGVPQGKALDLYEASPI 52
                 .***.*.*****.*.***..**.***.*.**.**...*....*****..****.

ba-MDH  61:QGFDANIIGTSDYADTADSDVVVITAGIARKPGMSRDDLVATNSKIMKSITRDIAKHSPN 120
gs-MDH  57:LGFDANIIGTSDYADTADSDIVVITAGIARKPGMSRDDLVTTNQKIMKQVTKEVVKYSPN 116
ca-MDH  53:EGFDVRVTGTNNYADTANSDVIVVTSGAPRKPGMSREDLIKVNADITRACISQAAPLSPN 112
             ***....**..*****.**..*.*.*..*******.**. .* .*.  .   .. ***

ba-MDH 121:AIIVVLTNPVDAMTYSVFKEAGFPKERVIGQSGVLDTARFRTFIAQELNLSVKDITGFVL 180
gs-MDH 117:CYIIVLTNPVDAMTYTVFKESGFPKNRVIGQSGVLDTARFRTFVAEELNISVKDVTGFVL 176
ca-MDH 113:AVIIMVNNPLDAMTYLAAEVSGFPKERVIGQAGVLDAARYRTFIAMEAGVSVKDVQAMLM 172
           . *....**.***** .....****.*****.****.**.***.* *.  ****......

ba-MDH 181:GGHGDDMVPLVRYSYAGGIPLETLIPKERLEAIVERTRKGGGEIVGLLGNGSAYYAPAAS 240
gs-MDH 177:GGHGDDMVPLVRYSYAGGIPLEKLIPKDRLDAIVERTRKGGGEIVNLLGNGSAYYAPAAS 236
ca-MDH 173:GGHGDEMVPLPRFSTISGIPVSEFIAPDRLAQIVERTRKGGGEIVNLLKTGSAYYAPAAA 232
           *****.****.*.*...***.. .*...** .**************.**..*********.

ba-MDH 241:LVEMTEAILKDQRRVLPAIAYLEGEYGYSDLYLGVPVILGGNGIEKIIELELLADEKEAL 300
gs-MDH 237:LVEMVEAILKDQRRILPAIAYLEGEYGYEGIYLGVPTILGGNGIEKVIELELLTEEEKAAL 296
ca-MDH 233:TAQMVEAVLKDKKRVMPVAAYLTGQYGLNDIYFGVPVILGAGGVEKILELPLNEEEMALL 292
           ...*.**.***..*..*..***.*.**. ..*.***.***..*.**..**.* ..*...*

ba-MDH 301:DRSVESVRNVMKVLV                                            315
gs-MDH 297:AKSVESVKNVMRMLE                                            311
ca-MDH 293:NASAKAVRATLDTLKSL                                          309
             *...*...  *
```

Fig. 2 Comparison of Mdh amino acid sequences. Identical and similar residues are indicated by asterisks and dots, respectively.

level of homology (estimated at 85.2% identity) with that of *B. anthracis* Mdh (ba-Mdh)[6]. gs-Mdh also exhibited relatively high homology with *C. auranti-acus* Mdh (ca-Mdh)[6] (57.9% identity). The open and closed forms of ba-Mdh and ca-Mdh have been well-characterized by X-ray crystallography (PDB ID: 3tl2 and 1uxi), with a high level of resolution (1.7 and 2.1 Å, respectively)[6]. Ideally, there would be no gaps in a pairwise alignment of gs-Mdh and ba-Mdh, and only one gap comprised of two residues was observed between gs-Mdh and ca-Mdh. In contrast, there were several gaps in pairwise alignment with the previous pm-Mdh base structure. Given that the catalytic functions of bacterial Mdhs have been sufficiently elucidated, the sequence and structural data were deemed useful as bases for homology modeling of gs-Mdh.

Molecular modeling of gs-Mdh

Three-dimensional models of gs-Mdh were constructed by computer analysis based on the ba-Mdh and ca-Mdh sequences and their X-ray crystallographic structures. Energy minimizations were applied to the models to further refine the structures. The open and closed molecular models of gs-Mdh were thus constructed by homology modeling using base structures with higher sequence identities. There were no outliers on the Ramachandran plot of

the open model, and only one outlier was observed on the plot of the closed model. This outlier, identified as residue N41, was found to be far from the active site and was located in an exposed loop at the protein surface. In contrast, the previously constructed model contained five outliers on the Ramachandran plot. The modeled three-dimensional structures of the present study were of much higher quality than the previous model and could thus enhance understanding of the structure-function relationship of gs-Mdh. The structures also provide a reliable basis for identifying sites for mutations to deliberately alter the enzyme's activity and stability.

Overall structures of monomers of the open and closed forms are presented in Figure 3. As expected, the three-dimensional structures of gs-Mdh are similar to those of other Mdh/Ldh family enzymes. The enzyme is composed of two domains, a catalytic and an NADH-binding domain. Two arginine residues, at positions 86 and 92, play an important role in substrate binding and change considerably in relative spatial position in the open and closed structures, whereas the catalytic residue H179 moves only minimally (Fig. 3). Residues R86 and R92 effectively create a positively charged cavity that stabilizes the carboxyl group of oxaloacetate by electrostatic interactions.

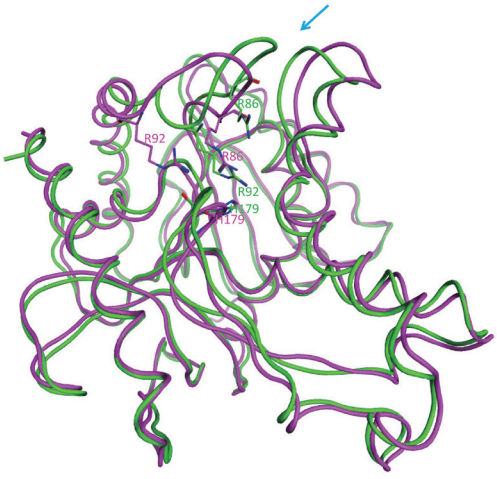

Fig. 3 Superposition of model structures of gs-Mdh. The superposition of open- and closed-forms, which are colored purple and green, respectively, was performed using the software MOE. The active site histidine and important arginine residues are represented as stick structures. The active site entrance is shown by arrow.

The open and closed forms of gs-Mdh superimpose well, with a root mean square deviation (RMSD) for atomic Cα positions of 1.3 Å. Superimpositions of the open form and ba-Mdh and the closed form and ca-Mdh yielded RMSDs for Cα positions of 0.54 and 0.70 Å, respectively. In contrast, superimposition of the closed form of the present study and the previously constructed models yielded an RMSD for Cα positions of 2.5 Å.

4. Discussion

To understand the difference in thermal stability at the structural level, the predicted number of hydrogen, ionic, and hydrophobic bonds was compared between the monomer proteins of gs-Mdh and ba-Mdh, which are typical thermophilic and mesophilic enzymes. The predicted number of hydrogen, ionic, and hydrophobic bonds in gs-Mdh/ba-Mdh was 87/65, 22/17, and 119/120, respectively. These data show that gs-Mdh contains a considerably larger number of hydrogen bonds than ba-Mdh (Fig. 4). In contrast, a recent structural analysis demonstrated that the high thermal stability of ca-Mdh is due to enhancement of subunit-subunit interactions[6]. Further investigations should be performed to determine whether the quaternary structure of gs-Mdh contributes to the enzyme's structural rigidity and stability.

Crystal structures of apo and substrate-bound forms of Mdhs have revealed slight movement of the binding loop structures around the substrate binding pocket. The motion of the binding loops may play a key role in substrate binding and subsequent enzyme activity. Estimation of the kinetic parameters of commercially available Mdhs based on Lineweaver-Burk plots returned K_m values of 5.0, 33, and 68 μmol/L for gs-Mdh, pm-Mdh, and tf-Mdh, respectively (Table 1). The substrate affinity of gs-Mdh is thus approximately 7-14 times higher than that of pm-Mdh and tf-Mdh. As discussed below, the different substrate affinities can be explained by comparing the active site structures of the enzymes.

Close-up view of the active site region of

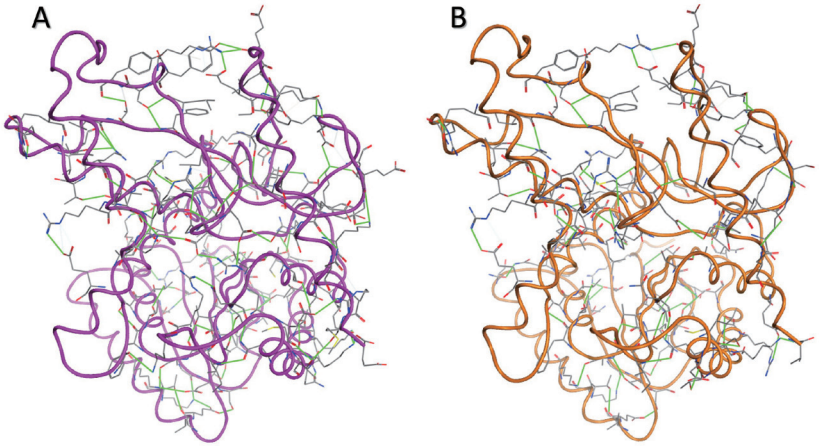

Fig. 4 Comparison between overall structures of thermophilic gs-Mdh (open-form, purple) and mesophilic ba-Mdh (orange). Hydrogen bonds predicted by the software MOE and related residues are represented as green lines and stick structures, respectively.

closed gs-Mdh was compared with that of closed pm-Mdh and tf-Mdh (Fig. 5A). Structural differences were observed around two large flexible loops at the entrance to the active site, although the residues important for substrate and NADH binding were conserved in each of the enzymes. The distance between the two loops was small in the closed form of gs-Mdh, consistent with the enzyme's high substrate affinity. In the tf-Mdh structure, the distance was extremely large, possibly because the enzyme was complexed with only a coenzyme NADH molecule. The active site spaces of the closed forms of gs-Mdh and pm-Mdh were also compared (Fig. 5B). Surface drawings indicated that the active site of pm-Mdh was wider than that of gs-Mdh.

In the previous study, two leucine residues of gs-Mdh were identified as important for oxaloacetate specificity[13]. These residues (L223 and L224) could cause steric interference in the enzyme-pyruvate interaction. Wild-type gs-Mdh exhibited no detectable activity with pyruvate. The hydrophobic and bulky side chains of both leucine residues, however, did not appear to interfere with pyruvate in the present closed model.

Residue R86 is known to be conserved in Mdhs and plays an important role in substrate specificity[1,2]. The residue at position 86 is also conserved in Ldhs as a glutamine, and Ldhs exhibiting pyruvate specificity can be easily converted to Mdhs by Q-to-R

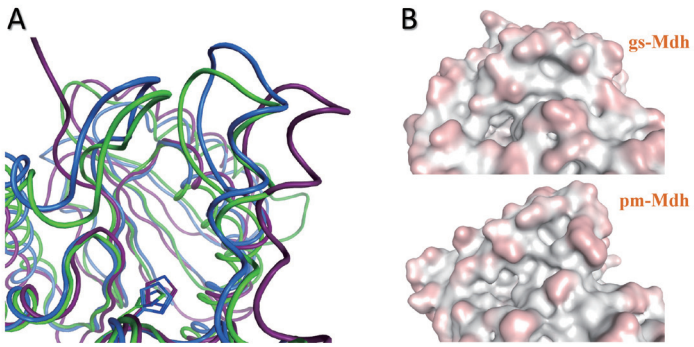

Fig. 5 Close-up views of the active site regions of Mdhs. (A) Superposition of gs-Mdh (closed-form, green), pm-Mdh (blue), and tf-Mdh (dark violet). The active site histidine residues are represented as stick structures. (B) Protein surface structures of gs-Mdh and pm-Mdh.

substitution[7,11]. These observations can be explained based on the role of the conserved arginine residue, which coordinates with the carboxyl group of oxaloacetate in Mdhs. An R86Q mutant of gs-Mdh was constructed using site-directed mutagenesis, as previously described. This mutant was not converted to an Ldh, although its activity toward oxaloacetate was markedly decreased. The mutational effect could not be clearly explained by the models. Superimposition of the closed forms of gs-Mdh and *G. stearothermophilus* Ldh[13] yielded an RMSD for Cα positions of 1.8 Å. Obtaining a more thorough understanding of the result may require the use of protein engineering techniques based on the model structures. Further investigations of the substrate specificity of gs-Mdh using site-directed mutagenesis and substrate-docking studies are now in progress.

References

1. Goward CR and Nichollsi DJ: Malate dehydrogenase: A model for structure, evolution, and catalysis. Protein Sci, 3: 1883-1888, 1994
2. Golding GB and Dean AM: The structural basis of molecular adaptation. Mol Biol Evol, 15:355-369, 1998
3. Chapman AD, Cortes A, Dafforn TR, Clarke AR, and Brady RL: Structural basis of substrate specificity in malate dehydrogenases: crystal structure of a ternary complex of porcine cytoplasmic malate dehydrogenase, alpha-ketomalonate and tetrahydoNAD. J Mol Biol, 285:703-712, 1999
4. Yin Y and Kirsch JF: Identification of functional paralog shift mutations: Conversion of *Escherichia coli* malate dehydrogenase to a lactate dehydrogenase. Proc Natl Acad Sci USA, 104: 17353–17357, 2007
5. Hung CH, Hwang TS, Chang YY, Luo HR, and Wu SP: Crystal structures and molecular dynamics simulations of thermophilic malate dehydrogenase reveal critical loop motion for co-substrate binding. PLoS One, 8: e83091, 2013
6. Kalimeri M, Girard E, Madern D, and Sterpone F: Interface matters: The stiffness route to stability of a thermophilic tetrameric malate dehydrogenase. PLoS One, 9: e113895, 2015
7. Wilks HM, Hart KW, Feeney R, Dunn CR, Muirhead H, Chia WN, Barstow DA, Atkinson T, Clarke AR, and Holbrook JJ: A specific, highly active malate dehydrogenase by redesign of a lactate dehydrogenase framework. Science, 242:1541-1544, 1988
8. Kallwass HKW, Luyten MA, Parris W, Gold M, Kay CM, and Jones JB: Effects of Gln102Arg and Cys97Gly mutations on the structural specificity and stereospecificity of the L-lactate dehydrogenase from *Bacillus stearothermophilus*. J Am Chem Soc, 114: 4551-4557, 1992
9. Kallwass HKW, Hogan JK, Macfarlane ELA, Martichonok V, Wendy, Parris W, Kay CM, Gold M, and Jones JB: On the factors controlling the structural specificity and stereospecificity of the L-lactate dehydrogenase from *Bacillus stearothermophilus*: Effects of Gln102Arg and Argl7lTrp/Tyr double mutations. J Am Chem Soc, 114: 10704-10710, 1992
10. Hogan JK, Carlos A. Pitto CA, Jones JB, and Gold M: Improved specificity toward substrates with positively charged side chains by site-directed mutagenesis of the L-lactate dehydrogenase of *Bacillus stearothermophilus*. Biochemistry, 34: 4225-4230, 1995
11. Hawrani ASE, Sessions RB, Moreton KM, and Holbrook JJ: Guided evolution of enzymes with new substrate specificities. J Mol Biol, 264:97-110, 1996
12. Nishiya Y: Enzyme design, protein design [Jpn]. Rinsyokensa, 46:853-859, 2002
13. Nishiya Y and Hirayama N: Molecular modeling and substrate binding study of the *Bacillus stearothermophilus* malate dehydrogenase. J Anal Bio-Sci, 23:117-122, 2000
14. Gleason WB, Fu Z, Birktoft J, and Banaszak L: Refined crystal structure of mitochondrial malate dehydrogenase from porcine heart and the consensus structure for dicarboxylic acid oxidoreductases. Biochemistry, 33:2078-2088, 1994
15. Kelly CA, Nishiyama M, Ohnishi Y, Beppu T, and Birktoft JJ: Determinants of protein thermostability observed in the 1.9-A crystal structure of malate dehydrogenase from the thermophilic bacterium *Thermus flavus*. Biochemistry, 32:3913-3922, 1993